JOURNAL OF APPLIED ELECTROCHEMISTRY 21 (1991) 753–759

Behaviour of a tall vertical gas-evolving cell Part II: Distribution of current

L. J. J. JANSSEN*, G. J. VISSER‡

Faculty of Chemical Technology and Computing Centre‡, Eindhoven University of Technology, P. O. Box 513, 5600 MB Eindhoven, The Netherlands*

Received 20 September 1990; revised 5 February 1991

Vertical electrolysers with a narrow electrode gap are used to produce gases, for example, chlorine, hydrogen and oxygen. The gas voidage in the solution increases with increasing height in the electrolyser and consequently the current density is expected to decrease with increasing height. Current distribution experiments were carried out in an undivided cell with two electrodes each consisting of 20 equal segments or with a segmented electrode and a one-plate electrode. It was found that for a bubbly flow the current density decreases linearly with increasing height in the cell. The current distribution factor increases with increasing average current density, decreasing volumetric flow rate of liquid and decreasing distance between the anode and the cathode. Moreover, it is concluded that the change in the electrode surface area remaining free of bubbles with increasing height has practically no effect on the current distribution factor.

Notation

A_e	electrode surface area (m^2)
$A_{e,s}$	surface area of an electrode segment (m^2)
$A_{e,1-19}$	total electrode surface area for the segments from 1 to 19 inclusive (m^2)
$A_{e,a}$	anode surface area (m^2)
$A_{e,a,h}$	$A_{e,a}$ remaining free of bubbles (m^2)
$A_{e,c}$	cathode surface area (m^2)
$A_{e,c,h}$	$A_{e,c}$ remaining free of bubbles (m^2)
a_1	parameter in Equation 7 (A^{-1})
B	current distribution factor
B_r	B in reverse position of the cell
B_s	B in standard position of cell
b_a	Tafel slope for the anodic reaction (V)
b_c	Tafel slope for the cathodic reaction (V)
d	distance (m)
d_{ac}	distance between the anode and the cathode (m)
d_{wm}	distance between the working electrode and an imaginary membrane (m) ($d_{wm} = 0.5\,d_{wt} = 0.5\,d_{ac}$)
d_{wt}	distance between the working and the counter electrode (m)
F	Faraday constant ($C\,mol^{-1}$)
h	height from the leading edge of the working electrode corresponding to height in the cell (m)
h_e	distance from the bottom to the top of the working electrode (m)
I	current (A)
I_s	current for a segment (A)
I_{20}	current for segment pair 20 (A)
I_{1-19}	total current for the segment pairs from 1 to 19 inclusive (A)
i	current density ($A\,m^{-2}$)
i_{av}	average current density of working electrode ($A\,m^{-2}$)
i_b	current density at the bottom edge of the working electrode ($A\,m^{-2}$)
i_0	exchange current density ($A\,m^{-2}$)
$i_{0,a}$	i_0 for anode reaction ($A\,m^{-2}$)
i_t	current density at the top edge of the working electrode ($A\,m^{-2}$)
n_1	parameter in Equation 15
n_s	number of a pair of segments of the segmented electrodes from their leading edges
Q_g	volumetric rate of gas saturated with water vapour ($m^3\,s^{-1}$)
Q_l	volumetric rate of liquid ($m^3\,s^{-1}$)
R	resistance of solution (Ω)
R_{20}	resistance of solution between the top segments of the working and the counter electrode (Ω)
R_p	resistance of bubble-free solution (Ω)
$R_{p,20}$	R_p for segment pair 20 (Ω)
r_s	reduced specific surface resistivity
$r_{s,0}$	r_s at $h = 0$
$r_{s,20}$	r_s for segment pair 20
$r_{s,\infty}$	r_s for uniform distribution of bubbles between both the segments of a pair
$r_{s,\infty,20}$	$r_{s,\infty}$ for segment pair 20
T	temperature (K)
U	cell voltage (V)
U_r	reversible cell voltage (V)
v_l	linear velocity of liquid ($m\,s^{-1}$)
$v_{l,0}$	v_l through interelectrode gap at the leading edges of both electrodes ($m\,s^{-1}$)
x	distance from the electrode surface (m)
β	gas volumetric flow ratio
β_{20}	β at segment pair 20
γ	specific surface resistivity ($\Omega\,m^2$)
γ_t	γ at top of electrode ($\Omega\,m^2$)

0021-891X/91 $03.00 + .12

γ_p γ for bubble-free solution (Ωm^2)
γ_b γ at bottom of electrode (Ωm^2)
δ thickness of Nernst bubble layer (m)
δ_0 δ at $h = 0$ (m)
$\delta_{0,i}$ δ_0 at i
ε voidage
$\varepsilon_{x,0}$ ε at x and $h = 0$
$\varepsilon_{0,0}$ voidage at the leading edge of electrode where $x = 0$ and $h = 0$
$\varepsilon_{0,0,i_b}$ $\varepsilon_{0,0}$ at i_b
$\varepsilon_{0,0,i_t}$ $\varepsilon_{0,0}$ at $i = i_t$
$\varepsilon_{\infty,h}$ voidage in bulk of solution at height h
$\varepsilon_{\infty,20}$ voidage in bubble of solution at the leading edge of segment pair 20
ε_{lim} maximum value of $\varepsilon_{0,0}$
η overpotential (V)
η_a anodic overpotential (V)
η_c cathodic overpotential (V)
η_h hyper overpotential (V)
$\eta_{h,a}$ anodic hyper overpotential (V)
$\eta_{h,c}$ cathodic hyper overpotential (V)
θ fraction of electrode surface area covered by of bubbles
θ_a θ for anode
θ_c θ for cathode
ρ resistivity of solution (Ωm)
ρ_p resistivity of bubble-free solution (Ωm)

1. Introduction

The current distribution over the gas-evolving electrodes in a rectangular cell is mainly determined by the distribution of voidage in the cell [1]. The kinetic parameters of the electrode reactions and the areas of the electrode surface which are free of bubbles are of particular interest.

To optimize a gas-evolving electrolyser, impedance and current distribution measurements have been carried out for an electrolysis of a 22 wt % NaOH solution in an undivided vertical electrolyser with a narrow inter-electrode gap. Results on cell impedance are published separately [2] and those on current distribution are presented in this paper.

The ohmic resistivity of the solution between the anode and the cathode during current flow increases continuously with increasing height in the electrolyser when the bubble–liquid mixture can be characterized by a bubbly flow [2]. Furthermore, the resistivity of the solution between the electrodes at the leading edge of both the electrodes increases practically linearly with the local current density, but the increase in solution resistivity at the bottom of the cell is larger than at the top of cell.

To obtain a well-based characterization of a gas-evolving electrolyser, current distribution measurements were carried under the same conditions as the impedance measurements. Results for the distribution in a gas-evolving diaphragm cell have been published by Bongenaar-Schlenter *et al.* [3, 4] and those in a hypochlorite electrolyser by Czarnetzki *et al.* [5, 6]. Further research has shown that, particularly at low current densities corresponding to low voidages, the reliability of the results is very sensitive to variations in the width of the inter-electrode gap.

2. Experimental details

2.1. *Experimental cell and electrodes*

The experimental set-up for a rectangular vertical cell has been described previously [5, 6]. Two types of nickel electrode were used, i.e. an electrode divided into 20 segments, each 0.010 or 0.020 m in width and 0.024 m in height, with a Perspex-filled space of 1 mm between successive segments and a one-plate electrode 0.020 m in width and 0.50 m in height. Experiments were carried out with two combinations of electrodes, namely, one with two segmented electrodes, both 0.01 m in width and the other combination with a segmented electrode and one-plate electrode, both 0.02 m in width.

The interelectrode gap d_{ac} was 3.2 mm for the experiments where both electrodes were segmented and varied between 1.0 and 7.0 mm for the experiments with the combination of a segmented electrode and a one-plate electrode. The width of the cell channel was equal to those of the electrodes used.

2.2. *Electrical measurements*

Two different constant-voltage sources with 20 independent channels (GEEST-1 and GEEST-2) were used: GEEST-1 for the combination of a segmented and a one-plate electrode and GEEST-2 for the combination of two segmented electrodes. Characteristics of GEEST-1 are given in [3–6] and those of GEEST-2 in [5]. The main difference between the two systems is the chargeability of segment pairs. Use of GEEST-2 allows the possibility of switching the current on or off through each pair of segments.

The experimental procedure with GEEST-1 is described in [5, 6] and that with GEEST-2 in [5]. Unless otherwise mentioned GEEST-2 was used. The relations between the current density, the cell voltage and the ohmic potential drop over the solution between the segments of a pair were determined with a Solatron 1250 frequency response analyser and a Solatron Electrochemical Interface 1286, as described in [2].

3. Results

3.1. *Relation between current density and cell voltage corrected for ohmic potential drop*

For a segment pair the ohmic potential drop, η_Ω, and the cell voltage, U, were determined with an impedance meter as a function of the current at various volumetric rates of liquid flow and at 323 K. Plotting $U - \eta_\Omega$ against log i it was found that for i in the

range from 2 to 8000 A m^{-2} the volumetric rate of liquid flow has no effect on the relation between i and $U - \eta_\Omega$. All the curves are straight and have the same slope. At 323 K the slope is 0.245 V.

For the cell action

$$H_2O \rightleftharpoons H_2 + \tfrac{1}{2}O_2$$

the reversible cell voltage was calculated as described in [7]. Calculation showed that the reversible cell voltage is 1.212 V, for a 22 wt% NaOH at 323 K. By linear extrapolation of the $(U - \eta_\Omega)/\log i$ curves it was found that the apparent exchange current density for the electrochemical decomposition of water is 0.98 A m^{-2}.

3.2. *Current distribution*

3.2.1. Introduction. To obtain reproducable results for current distribution, a pre-electrolysis was necessary for at least 30 min. Using GEEST-2 the current distribution over the segmented cathode as well as the segmented anode was measured 5 times, alternately, at $I_{1\text{-}19} = 25$ A and $Q_1 = 6.0 \times 10^{-6}$ m^3 s^{-1}. A typical result is given in Fig. 1. This shows the ratio $I_s/I_{s,av}$ as a function of the number of segment, n_s, for the segmented cathode as well as the segmented anode. Figure 1 also indicates clearly that the current distributions over both types of gas-evolving electrodes are practically the same. Consequently, the cell-current distribution is equal to those over both the electrodes for a gas-evolving tall vertical cell with a small inter-electrode gap.

Moreover, Fig. 1 shows that the fluctuations in the curve for the hydrogen-evolving electrode are clearly larger than those for the oxygen-evolving electrode. This difference may be caused by a difference in the Tafel slope for hydrogen and for oxygen evolution on nickel in concentrated alkaline solution. The Tafel slopes were 0.14 V and 0.095 V, respectively, for hydrogen and oxygen evolution on nickel in 50 wt% KOH at 353 K [7].

Current distribution curves were usually linear. Only at low Q_1 and high $I_{1\text{-}19}$ were the current distribution curves slightly curved; the current density decreasing at a decreasing rate with increasing height in the cell.

The deviation from the linear I_s/n_s curve becomes significant at a gas volumetric flow ratio β, defined as $Q_g/(Q_g + Q_l)$, greater than ~ 0.65. We observed a transition from a bubbly flow to a slug flow [8] at the same β.

From the I_s/n_s line the current density at the top, i_t, and that at the leading edge of the electrode, i_b, were obtained by linear extrapolation. From these values the current distribution factor $B = (i_b - i_t)/i_{av}$ was calculated. The slope of the I_s/n_s curve was determined by linear regression. The accuracy in B increases strongly with increasing current $I_{1\text{-}19}$. Particularly, the inaccuracy in B was large at low $I_{1\text{-}19}$, for instance 1 A.

3.2.2. Effect of cell position. Since it is likely that the distance between the electrodes is not constant for the whole height of the cell and the surface areas of the segments and the potential difference between two opposite segments can vary, a series of experiments was carried out with the cell in the standard as well as in the reverse position. Consequently, the systematic error in the current distribution factor due to the above mentioned factors was eliminated.

Figure 2 shows the current distribution factor B_s and B_r as a function of the total current $I_{1\text{-}19}$ for the cell in both positions where B_s is B for the standard

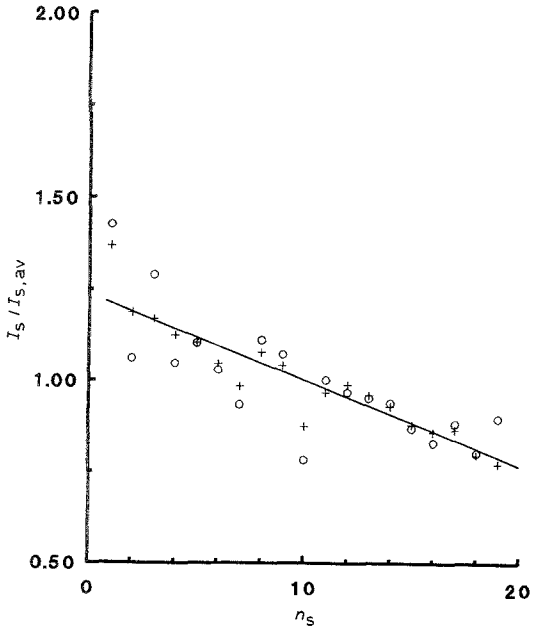

Fig. 1. Segment current ratio $I_s/I_{s,av}$ for the segmented anode (+) as well as the segmented cathode (○) is plotted as a function of the segment number n_s. The electrolysis conditions: current $I_{1\text{-}19}$ is 25 A, temperature is 323 K, the volumetric flow rate of liquid is 6.0 × 10^{-6} m^3 s^{-1}.

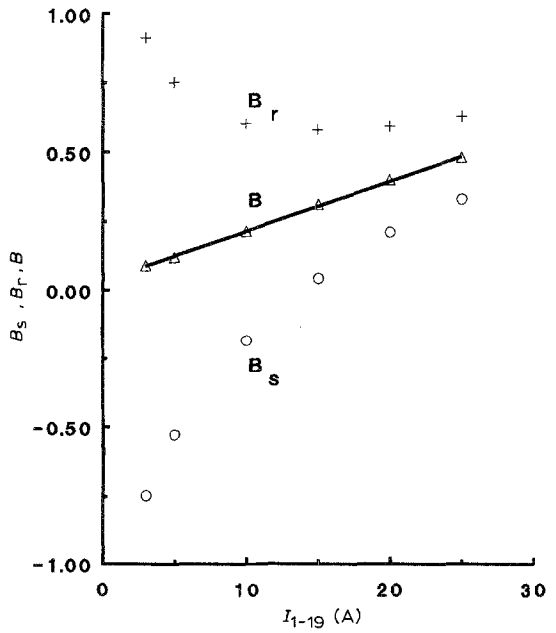

Fig. 2. The distribution factors B, B_s and B_r as a function of $I_{1\text{-}19}$ for a cell with segmented electrodes at a temperature of 323 K, a volumetric flow rate of liquid of 6 × 10^{-6} m^3 s^{-1} and an inter-electrode gap width of 3.2 mm. The distribution factor $B = (B_s + B_r)/2$.

position and B_r for the reverse position of the cell. The curves differ significantly. A $B/I_{1\text{-}19}$ curve for an ideal configuration of the cell and at the same difference in potential for each segment pair is obtained from both curves, where $B = (B_s + B_r)/2$.

From Fig. 2 it follows that the $B/I_{1\text{-}19}$ curve intersects the origin of the $B/I_{1\text{-}19}$ plot and B is proportional to $I_{1\text{-}19}$.

It was shown that the increasing divergence of both curves in Fig. 2 is not caused by the inequality in the potential differences for the segment pairs. These potential differences were measured for various $I_{1\text{-}19}$ and the effect on the current distribution was calculated.

3.2.3. Effect of the volumetric rate of gas flow and of liquid flow. Figure 2 shows the effect of $I_{1\text{-}19}$ or the volumetric rate of gas flow on the current distribution factor, B, for the combination of segmented electrodes and measured with GEEST-2. It shows that the current distribution factor increases linearly with increasing current density $I_{1\text{-}19}$ and with increasing gas volumetric flow rate. The effect of the liquid volumetric flow rate on the current distribution factor at $I_{1\text{-}19} =$ 25 A is shown in Fig. 3. This shows that the absolute value of the current distribution factor decreases at a decreasing rate with increase in liquid volumetric flow rate.

The effect of volumetric rate of the gas flow and that of the liquid flow on the current distribution factor were also determined for the combination consisting of a segmented electrode and a one-plate electrode. These measurements were carried out with GEEST-1. The results are presented in Fig. 4 for various volumetric rates of liquid flow for an anode to cathode distance, d_{ac}, of 4 mm. This figure shows a deviation of the linear B/I_t dependence simultaneously at a low Q_l and a high I_t corresponding to a gas volumetric flow ratio β greater than ~ 0.6.

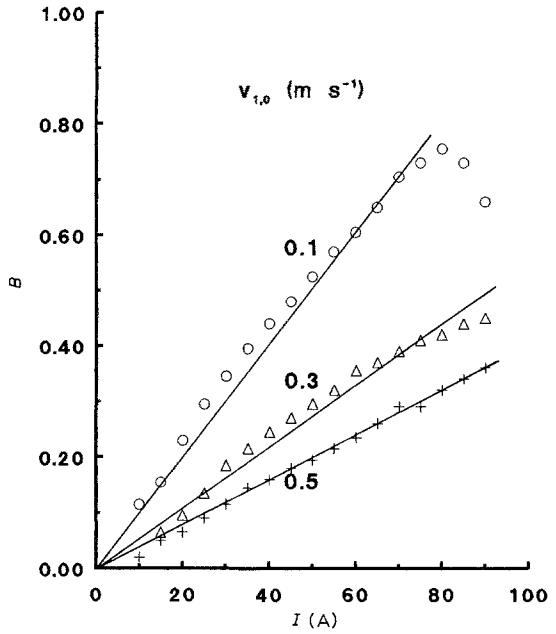

Fig. 4. The distribution factor B as a function of total current I_t for a cell with a combination of a segmented electrode and a one-plate electrode at various volumetric rates of liquid flow, an inter electrode gap width of 4.0 mm and a temperature of 343 K.

3.2.4. Effect of temperature. Heat is evolved in the electrolyser during current flow. The difference in temperature of the solution at the outlet and inlet of the cell is negligible at temperatures greater than ~ 313 K. Temperatures above 343 K could not be used because of the nature of the cell material. In Fig. 5 the current distribution factor, B, is plotted as a function of the temperature for the cell with the segmented electrodes. This shows that B increases with increasing temperature.

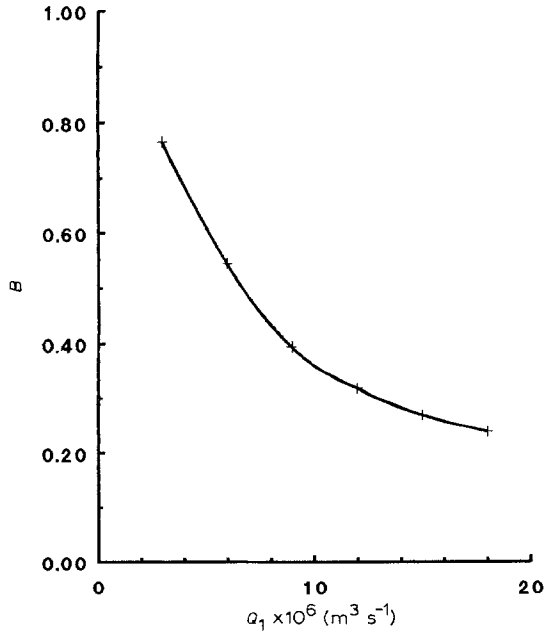

Fig. 3. The distribution factor B as a function of the volumetric rate of liquid flow for a cell with segmented electrodes at various $I_{1\text{-}19}$, a temperature of 323 K and an inter-electrode gap width of 3.2 mm.

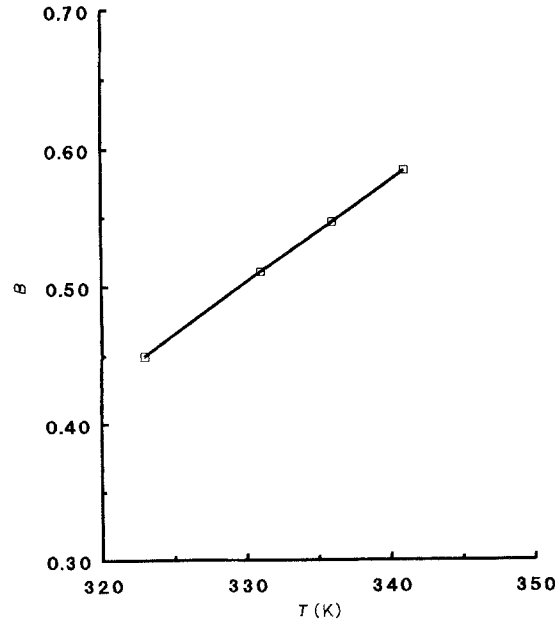

Fig. 5. The distribution factor B as a function of temperature for a cell with a combination of two segmented electrodes at $I_{1\text{-}19} = 25$ A, $Q_l = 6.0 \times 10^{-6}$ m^3 s^{-1} and an inter-electrode gap width of 3.2 mm.

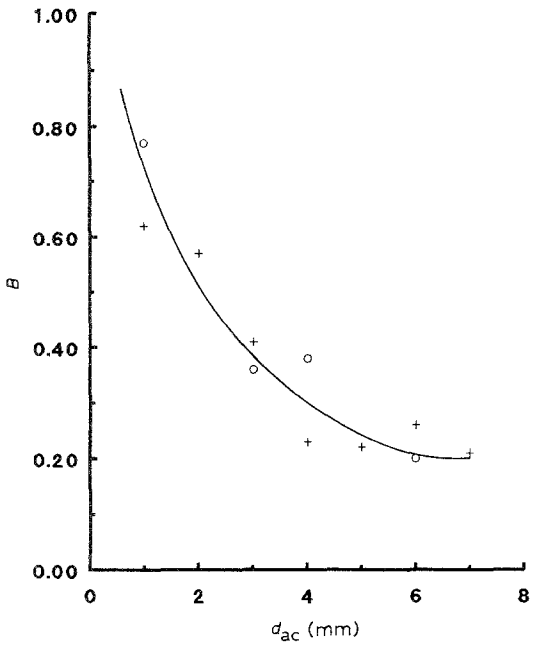

Fig. 6. The distribution factor B for two series of experiments as a function of the width of the inter electrode gap for a cell with a segmented electrode and a one plate electrode at $I_t = 70$ A, 343 K and a velocity of solution $v_0 = 0.3\,m\,s^{-1}$; (O) indicated an average B obtained from experiments with the cell in standard as well as in reverse position, and (x) indicated a single B obtained from experiments with the cell in standard position.

3.2.5. Effect of the distance between anode and cathode. The constant-voltage source GEEST-1 was used to determine the effect of the distance d_{ac} between both electrodes on the current distribution. The cathode was the segmented plate-electrode and the anode and one-plate electrode and *vice versa*. It was found that the current distribution does not depend on the direction of electric current through the cell. Experiments were carried out at 343 K, $I_t = 70$ A and at a liquid velocity of $0.30\,m\,s^{-1}$ through the cross-section of the cell at the leading edge of both electrodes. The results are plotted in Fig. 6. From this it follows that the factor B decreases at a decreasing rate with increasing distance d_{ac}.

4. Discussion

When the bubble-liquid mixture can be characterized by a bubbly form – in which the liquid phase is continuous and the gas-vapour phase is discontinuous and the gas-vapour phase is distributed in the liquid in the form of bubbles – the current density decreases linearly with increasing height in the oxygen and hydrogen-evolving cell (§3.1.2). The decrease in the current density with increasing height in the cell is expressed by the current distribution factor B. This is zero when the current is uniformly distributed over the electrode.

From Fig. 1 it follows that the current distribution over the segmented nickel anode is equal to that over the segmented nickel cathode. It can be concluded that for a tall rectangular cell with a narrow gap the current distribution is the same for each vertical cross-section, where the edge effects are neglected.

Current distribution depends on the kinetic parameters of the electrode reactions, the electrode-surface areas remaining free of bubbles and on the ohmic resistivity of the solution between the electrodes. The cell voltage, U, is the sum of the reversible cell voltage, U_r, the anode overpotential, $\eta_a = b_a \log |i|$, the cathode overpotential, $\eta_c = b_c \log |i|$, the specific surface resistivity of the solution between the electrodes, γ_s, and the hyperovervoltage or hyperpolarization, η_h, at the anode and cathode.

The term "hyperpolarization" introduced by Leistra and Sides [9] is the overpotential due to the masking of the electrode by bubbles. The hyperoverpotential at the anode and cathode is given by, respectively, $\eta_{h,a} = b_a \log (A_{e,a}/A_{e,a,h})$ and $\eta_{h,c} = b_c \log (A_{e,c}/A_{e,c,h})$, where $A_{e,a,h}$ and $A_{e,c,h}$ are, respectively, the anode surface area and cathode surface area remaining free of bubbles during gas evolution [9]. The ratio $A_{e,h}/A_e$ can be replaced by $1 - \theta$, where θ is the fraction of the electrode surface area covered by bubbles.

The cell voltage is given by

$$U = U_r + b_a \log \frac{|i|}{i_{0,a}} + b_c \log \frac{|i|}{i_{0,c}} - b_a \log (1 - \theta_a) - b_c \log (1 - \theta_c) + i\gamma_s \quad (1)$$

When the cell voltage is constant over the height of the electrode, the difference between the current density at the bottom and at the top can be calculated from the relation

$$(b_a + b_c) \log \left(\frac{i_b}{i_t}\right) = b_a \log \left(\frac{1 - \theta_{a,b}}{1 - \theta_{a,t}}\right) + b_c \log \left(\frac{1 - \theta_{c,b}}{1 - \theta_{c,t}}\right) + i_t\gamma_t - i_b\gamma_b \quad (2)$$

For oxygen evolution on a nickel electrode in 0.5 M NaOH and at $1\,kA\,m^{-2}$ Leistra and Sides [9] have found that the hyperovervoltage is 3 mV corresponding to a 7% reduction in effective electrode surface area by the oxygen bubbles. For hydrogen evolution the hyperovervoltage is even smaller, due to the smaller bubble size [9].

It is likely that the hypervoltage depends on the voidage at the electrode surface. For a gas-evolving cell with a uniform current distribution the voidage in the solution is given by [2]

$$\varepsilon_{x,h}^4 = \varepsilon_{0,0}^4 \left(1 - \frac{x}{\delta_0}\right)^4 + \varepsilon_{\infty,h}^4 \quad (3)$$

where $\varepsilon_{x,h}$ is the voidage in the solution at a distance x from the working electrode and a height h from its leading edge; $\varepsilon_{0,0}$ is the voidage in the solution at $x = 0$ and $h = 0$; $\varepsilon_{\infty,h}$ is the voidage in the bulk of solution at a height h; and δ_0 is the thickness of Nernst bubble layer at $h = 0$.

The voidage $\varepsilon_{0,h}$ at the electrode surface as a function of the height in a gas-evolving cell with a uniform current distribution follows from Equation 3 and is

given by

$$\varepsilon_{0,h}^4 = \varepsilon_{0,0}^4 + \varepsilon_{\infty,h}^4 \quad (4)$$

However, the local current density decreases with increasing height (Fig. 1). This means that the increase in $\varepsilon_{0,h}$ with increasing height is smaller than that calculated with the above mentioned relation for $\varepsilon_{0,h}$. So, in practice, $\varepsilon_{0,h}$ is practically independent of height in the cell.

It is likely that the electrode surface area available for current flow is proportional to $1 - \varepsilon_{0,h}$. This means that the change in the electrode surface area to current flow with increasing height in the cell is small and has only a small effect on the current distribution. Consequently, Equation 2 may be simplified to

$$(b_a + b_c) \log (i_b/i_t) = i_t\gamma_t - i_b\gamma_b \quad (5)$$

In the following the ratio γ_t/γ_b has been calculated for the electrolysis of a 22 wt %. NaOH solution with nickel electrodes (0.475 m in height) in an undivided cell at $d_{ac} = 3.2$ mm, $Q_l = 6.0 \times 10^{-6}$ m^3 s^{-1}, $T = 323$ K and at various $I_{l\text{-}19}$. The experimental distribution factor B at various $I_{l\text{-}19}$ are given in Fig. 2 and Table 1. From the factor B the current densities i_b and i_t are calculated using, respectively, $i_b = i_{av} + \frac{1}{2}Bi_{av}$ and $i_t = i_{av} - \frac{1}{2}Bi_{av}$. Using the relation for i_b, $\gamma_b = \gamma_p (1 + 0.515 \times 10^{-4} i_b)$ (Fig. 4 from [2]) and $\gamma_p = 0.4464 \times 10^{-4}\,\Omega$m^2 (calculated from $R_{p,20} = 0.186\,\Omega$ and $A_e = 2.4 \times 10^{-4}$ m^2 [2]), γ_b at various i_{av} has been calculated. The results are provided in Table 1.

Using Equation 2, the results for i_b, i_t and γ_b and the sum $b_a + b_c = 0.245$ V, the parameters γ_t and γ_t/γ_b at various i_{av} have been calculated and given in Table 1. Also, the experimental γ_t/γ_b values obtained from the results given in [2, Fig. 2] have been tabulated.

It should be noted that $\gamma_t = \gamma_p r_{20}$ at $I_{20} = i_t A_{e,s}$ and $I_{l\text{-}19} = i_{av} A_{e,l\text{-}19}$ and $\gamma_b = \gamma_p r_{20}$ at $I_{20} = i_b A_{e,s}$ and $I_{l\text{-}19} = 0$ A.

Comparing the calculated and the experimental ratio γ_t/γ_b it follows that both ratios are practically the same. Consequently, the current distribution in the cell agrees very well with the increase in the specific surface resistivity with increasing height in the cell and that a possible change in the electrode surface area remaining free of bubbles with increasing height in the cell does not affect the current distribution in the cell significantly.

Table 1.

$I_{l\text{-}19}$ (A)	i_{av} (A m^{-2})	B (−)	$\gamma_b \times 10^{-4}$ (Ω m^2)	$\gamma_t \times 10^4$ (Ω m^2)	γ_t/γ_b (*)	γ_t/γ_b (†)
25	5480	0.48	0.603	1.108	1.84	1.80
20	4386	0.40	0.567	0.973	1.71	1.69
15	3289	0.30	0.533	0.836	1.57	1.58
10	2193	0.21	0.502	0.721	1.44	1.43
5	1096	0.12	0.473	0.657	1.39	1.26

* calculated
† experimental.

From these results it follows that the current distribution in the cell can be calculated using Equation 5.

The sum $b_a + b_c$ is determined by both electrode reactions. The specific ohmic resistivity as a function of the height in the cell can be obtained from the Bruggeman relation using the specific ohmic resistivity of the bubble-free solution and the distribution of the voidage in the cell.

For a uniform distribution of current the voidage distribution is described by Equation 3. The determination of $\varepsilon_{x,h}$ is extensively described in [2]. In practice, the effect of the non-uniform distribution of current has to be taken into account to calculate the voidage distribution in a gas-evolving cell.

This means that Equation 3 has to be changed to

$$\varepsilon_{x,h}^4 = \varepsilon_0^{*4}\left(1 - \frac{x}{\delta_{0,h}^*}\right)^4 + \varepsilon_{\infty,h}^4 \quad (6)$$

where

$$\varepsilon_{0,h}^* = \varepsilon_{0,0} \text{ at } i_h$$
$$\delta_{0,h}^* = \delta_0 \text{ at } i_h$$

For bubbly flow the maximum voidage is about 0.65 [§3.1.2]. This maximum agrees reasonable with the maximum voidage which can be derived for various lattice types of bubble arrangement. For instance, for a simple cubic, a face-centred and a body-centred cubic structure the maximum voidages are 0.52, 0.74 and 0.68, respectively [10]. From the experimental results of [2]

$$\varepsilon_{0,0}/(0.65 - \varepsilon_{0,0}) = a_l i_b \quad (7)$$

and consequently

$$\varepsilon_{0,t}^*/(0.65 - \varepsilon_{0,t}^*) = a_l i_t \quad (8)$$

To calculate numerically the current distribution factor from the results of impedance measurements various relations have to be used. These are Equations 5 to 8 and the relations:

$$i_b = (1 + 0.5B)\, i_{av} \quad (9)$$

$$i_t = (1 - 0.5B)\, i_{av} \quad (10)$$

$$\gamma_b = 2\rho_p d_{wm} r_{s,0} \quad (11)$$

where

$$r_{s,0} = \frac{1}{d_{wm}} \int_0^{\delta_0} (1 - \varepsilon_{x,0})^{-1.5}\, dx + \left(\frac{d_{wm} - \delta_0}{d_{wm}}\right) \quad (12)$$

being Equation 7 from [2], and

$$\gamma_t = 2\rho_p d_{wm} r_{s,t} \quad (13)$$

where

$$r_{s,t} = \frac{1}{d_{wm}} \int_0^{\delta_{0,t}^*} (1 - \varepsilon_{x,t})^{-1.5}\, dx + (1 - \varepsilon_{\infty,t})^{-1.5}\left(\frac{d_{wm} - \delta_{0,t}^*}{d_{wm}}\right) \quad (14)$$

being similar to Equation 10 from [2].

The calculation has been carried out for $b_a +$

$b_c = 0.245\,V$ [§3.1], $\rho_p = 0.01395\,\Omega m$ [2], $I_{1\text{-}19} = 25\,A$ ($i_{av} = 5482\,A\,m^{-2}$), a solution bulk velocity through the cross-section of the cell at the level of the leading edge of both electrodes $v_{1,0} = 0.188\,m\,s^{-1}$, a temperature of 323 K, $d_{wm} = 1.6\,mm$, $d_{ac} = 3.2\,mm$ and $\delta_0 = 2.4 \times 10^{-6}\, i_b^{0.6}$ [2] and $\delta^*_{0,t} = 2.4 \times 10^{-6}\, i_t^{0.6}$. To calculate the voidage of bulk solution at the top of electrode, the vapour pressure for the 22 wt % NaOH solution, a total pressure of 1.082 atm at the level of the top of electrode and the slip factor for bubbles [2] have been taken into account. It has been found that $B = 0.48$ for the cell with a height of 0.475 m and for the above mentioned electrolytic conditions. The experimental value at $I_{1\text{-}19} = 25\,A$ is 0.46 (Table 1). It may be concluded that the agreement between the experimental and calculated result is good.

The current distribution factor can also be calculated for very simplified models. These calculations provide good insight into the effect of several factors.

The calculations were carried out for the electrolysis at $I_{1\text{-}19} = 25\,A$ for which the experimental $B = 0.46$ (Table 1). For the simplifed models where the evolved bubbles are uniformly distributed over the horizontal cross section of the cell and the voidages are equal to the gas volumetric flow ratio and the bulk voidage used for the advanced model, the current distribution factors are 0.70 and 0.64, respectively.

For the advanced model and using results of impedance measurements, the calculated $B = 0.48$. From this difference in current distribution factors it follows that the bubble-slip ratio can significantly affect the current distribution factor. An increasing bubble-slip ratio produces a more uniform current distribution over the cell. From the large difference between the calculated B for the advanced model and the calculated values for the simplified models it follows that the bubble-layers at the electrodes strongly affect the current distribution over the cell.

The effect of the inter-electrode-gap width, d_{ac}, on the current distribution factor was numerically calculated for the electrolysis of a 22 wt % NaOH solution in an undivided cell with $w_e = 10.0\,mm$, $h_e = 0.475\,m$ and d_{ac} varying from 1 to 100 mm and at $I_{1\text{-}19} = 25\,A$ corresponding to $i_{av} = 5482\,A\,m^{-2}$, $v_{1,0} = 0.188\,m\,s^{-1}$ and $T = 323\,K$. The method of calculation for $d_{ac} = 3.2\,mm$ has already been described in this section. The result is given by curve a in Fig. 7. It is evident that the electrochemical parameters b_a and b_c, the relation between $\varepsilon_{0,0}$ and current density and that between δ_0 and current density do not depend on d_{ac} at the same liquid velocity. Plotting the experimental results given in Fig. 6 on a double logarithmic scale as in Fig. 7 it can be seen that the experimental relation between B and d_{ac} agrees reasonably with the theoretical results.

The resistivity of the bubble-free solution clearly affects the distribution of current in the cell. To show this effect, the calculations were carried out for solutions ρ_p and where the other parameters are equal to

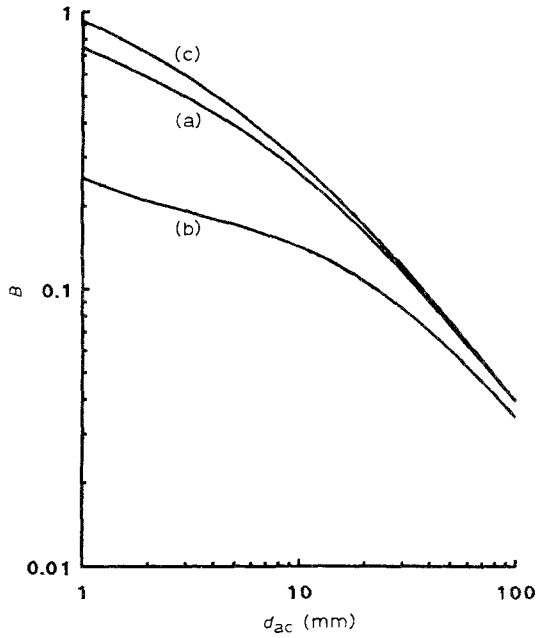

Fig. 7. The calculated distribution factor B plotted versus the width of the inter-electrode gap on a double logarithmic scale for water electrolysis in 22 wt % NaOH at $T = 323\,K$, $i_{av} = 5482\,A\,m^{-2}$ and $v_{1,0} = 0.188\,m\,s^{-1}$ (a). The resistivity of the bubble-free solution is $0.01395\,\Omega m$ for curve a, $0.001395\,\Omega m$ for curve b and $0.1395\,\Omega m$ for curve c. Experimental results for $d_{wt} = 3.2\,mm$ were used.

those for curve a. The results for $\rho_p = 0.001395$ and $0.1395\,\Omega m$ are given by curve b and c, respectively, in Fig. 7. From Fig. 7 it follows, that the absolute value of the current distribution factor increases with increasing resistivity of the bubble-free solution. Fig. 5 shows that the absolute value of the current distribution factor increases with increasing temperature and thus, with decreasing resistivity of the bubble-free solution. Consequently, other factors, such as the vapour pressure and bubble behavior, have an opposite effect.

References

[1] H. Vogt in E. Yeager, J. O'M. Bockris, B. E. Conway and S. Sarangapani, 'Comprehensive treatise of Electrochemistry', Plenum Press, New York (1983), vol. 6, p. 476.
[2] L. J. J. Janssen and G. J. Visser, *J. Appl. Electrochem.* **21** (1991) 386.
[3] B. E. Bongenaar-Schlenter, Ph.D. Thesis, Eindhoven University of Technology, Eindhoven (1984).
[4] B. E. Bongenaar-Schlenter, L. J. J. Janssen, S. J. D. van Stralen and E. Barendrecht, *J. Appl. Electrochem.* **15** (1985) 537.
[5] L. R. Czarnetzki, Ph.D. thesis, Eindhoven University of Technology, Eindhoven (1989).
[6] L. R. Czarnetski and L. J. J. Janssen, *J. Appl. Electrochem.* **19** (1989) 630.
[7] M. H. Miles, G. Kessel, P. W. T. Lu and S. Srinivasan, *J. Electrochem. Soc.* **123** (1976) 322.
[8] L. S. Tong, 'Boiling Heat Transfer and Two-Phase Flow', John Wiley and Sons, New York (1965), p. 47.
[9] J. A. Leistra and P. J. Sides, *Electrochim. Acta* **32** (1987) 1489.
[10] G. Kreysa and M. Kuhn, *J. Appl. Electrochem.* **15** (1985) 517.